Solvent Effects on the Kinetics and Thermodynamics of Stacking in Poly(cytidylic acid)†

Susan M. Freier, K. O. Hill, T. G. Dewey, Luis A. Marky, Kenneth J. Breslauer, and Douglas H. Turner*

ABSTRACT: The Raman laser temperature-jump technique has been used to measure the kinetics of the coil to helix reaction of poly(cytidylic acid) [poly(C)] in aqueous cosolvent mixtures. The rate of helix formation has a low activation energy and is proportional to reciprocal solvent viscosity. The observations suggest helix formation is rotationally diffusion controlled. The rate of coil formation in poly(C) has an activation energy of ~11 kcal/mol, presumably reflecting the electronic stacking interactions which stabilize the helix. Viscous cosolvents, glycerol or sucrose, slow down the rate of coil formation; acetonitrile and formamide at 5 mol % increase the rate relative to that in water. The polar cosolvents may specifically attack a cytosine stack. The absorbance vs. temperature profiles for poly(C) are analyzed with the one-dimensional Ising model. When only optical data are used, the cooperativity parameter, σ, and the enthalpy, ΔH, cannot be uniquely determined. A method is proposed that allows determination of σ by combining spectroscopic and calorimetric data. The values of σ derived for poly(C) are between 0.8 and 1.0, and ΔH is about −9 kcal/mol of stack. An alternative method using integration of the excess heat capacity curve and extrapolation to fully stacked and random coil species yields a ΔH of −7 kcal/mol of stack.

One of the major forces thought to stabilize helical structure in nucleic acids is the base–base stacking interaction (Crothers & Zimm, 1964; Cantor & Schimmel, 1980). The nature of the forces dominating this interaction is not well understood. Both electronic and solvent forces are thought to be important (Pullman & Pullman, 1968, 1969; Lawaczeck & Wagner, 1974; Sinanoğlu & Abdulnur, 1965; Sinanoğlu, 1968; Cantor & Schimmel, 1980). The effects of solvent on the interaction should aid in characterization of these forces.

Some single-stranded polynucleotides form helical structures (Felsenfeld & Miles, 1967; Arnott et al., 1976) and provide simple models for stacking in nucleic acids. The dynamics of this process for polyadenylic acid [poly(A)][1] and polycytidylic acid [poly(C)] have been studied in water (Pörschke, 1973, 1976, 1978; Dewey & Turner, 1979), and poly(A) has been studied in aqueous solvent mixtures (Dewey & Turner, 1980). This paper reports the equilibrium and kinetic effects of solvent mixtures on poly(C) stacking.

Experimental Procedures

Poly(C). Solutions of poly(C) (Sigma Chemical Co.) were prepared by extensive dialysis at 4 °C against a solution containing 0.001 M EDTA and 0.05 M sodium cacodylate, pH 7.0, followed by dialysis against 0.05 M sodium cacolyate, pH 7.0. To check for hydrolysis of the polymer, we ran gel electrophoresis on samples before and after a temperature-jump or melting experiment. In 10% polyacrylamide gel (DeWachter & Fiers, 1971), the samples ran slower than a poly(A) marker of average length 410 nucleotides (Miles). No change in mobility was observed after a temperature-jump or melting experiment.

Cosolvents. Formamide was purified by recrystallization (Casey & Davidson, 1977). All other cosolvents were the highest quality available and used without further purification. The absorbance of the mixed solvents at 280 nm was <0.02 cm^{-1}.

Melting Curves. The temperature dependence of the absorbance at 280 nm was measured in a Gilford 250 spectrophotometer interfaced to a PDP 11/34 computer. The spectral bandwidth was 2.2 nm. The temperature was varied continuously from 0 to 88 °C at 30 °C/h. To assure uniform heating of the samples containing glycerol and sucrose, we reduced the heating rate to 12 °C/h and used 0.1-cm path length cells instead of 1-cm cells.

Spectra. Circular dichroism spectra were measured with a Jasco J-40 spectropolarimeter and absorption spectra with a Cary 219 spectrophotometer. Concentrations were calculated by assuming $\epsilon_{274} = 7.7 \times 10^3$ M^{-1} cm^{-1} for poly(C) at 2 °C in 0.05 M sodium acetate, pH 4.0 (Akinrimisi et al., 1963), and $\epsilon_{268} = 6.1 \times 10^3$ M^{-1} cm^{-1} for poly(C) at 2 °C in 0.05 M sodium cacodylate, pH 7.0 (Brahms et al., 1967). The extinction was assumed to be independent of solvent for the calculation of $\Delta\epsilon$ in mixed solvents.

Calorimetry. The differential scanning calorimetry (DSC) was performed with a Microcal-1 instrument as previously described (Albergo et al., 1981). In a typical experiment, the temperature was scanned from 15 to 95 °C at a rate of 0.95 °C/min. The buffer was 0.01 M sodium phosphate, 0.001 M EDTA, and 0.2 M NaCl, pH 7 (calorimetry buffer), and the poly(C) concentration ranged from 11 to 24 mM. The latter concentrations were determined by using $\epsilon_{269} = 6.3 \times 10^3$ M^{-1} cm^{-1} at 20 °C (Adler et al., 1967).

Kinetics. The kinetics were measured by using a laser temperature-jump apparatus (Dewey & Turner, 1978; Turner et al., 1972). A 2-ms high current pulse was applied to the xenon lamp to increase light intensity (Turner et al., 1974). A photographic shutter limited sample exposure to 20 ms/temperature jump.

† From the Department of Chemistry, University of Rochester, Rochester, New York 14627 (S.M.F., K.O.H., T.G.D., and D.H.T.), and the Department of Chemistry, Douglass College, Rutgers University, New Brunswick, New Jersey 08903 (L.A.M. and K.J.B.). *Received June 19, 1980; revised manuscript received November 25, 1980.* This work was supported by National Institutes of Health Grants GM 22939 and GM 23509. D.H.T. is an Alfred P. Sloan Fellow. T.G.D. was a National Institutes of Health Predoctoral Trainee (Grant 5T32GM07230).

[1] Abbreviations used: poly(A), poly(adenylic acid); poly(C), poly(cytidylic acid); poly(I), poly(inosinic acid); CMP, cytidine monophosphate; EDTA, ethylenediaminetetraacetate; EtOH, ethanol; MeOH, methanol; PrOH, 1-propanol; CD, circular dichroism; DSC, differential scanning calorimetry; RNA, ribonucleic acid; DNA, deoxyribonucleic acid.

0006-2960/81/0420-1419$01.25/0

Relaxations were measured at 275 or 280 nm. For poly(C) in 0.05 M sodium cacodylate, pH 7.0, at 30 °C, the relaxation time was measured at 260 nm as well as at 280 nm. Identical relaxation times were obtained at both wavelengths. The monochromator between the xenon lamp and the sample had a 16-nm spectral bandwidth. Schott UG 11 and UG 5 filters or an Acton Research Corporation 260-nm (36-nm band-pass) interference filter was placed in front of the phototube. Signals with the Schott filters were similar to those with the interference filter. The reported relaxation times and estimated errors are the average and standard deviation, respectively, obtained from at least 15 measurements.

To test for photochemical effects, we measured the signal from poly(C) in D_2O. The temperature jump in D_2O is 100 times less than that in H_2O. No signal was observed with salt concentrations of 0.05 or 1.0 M.

Results

Temperature Dependence of UV Absorption Spectra. The absorption spectrum of 5′-CMP shows a strong temperature dependence. If corrections are not made for volume expansion, there are apparent isosbestic points at 252 and 280 nm (Pörschke, 1976). This indicates that at these wavelengths, the volume expansion compensates for a temperature-dependent extinction coefficient. This temperature-dependent extinction has been attributed to dissociation of solvent molecules hydrogen bonded to cytosine (Johnson et al., 1971). A similar temperature dependence of the absorption spectrum is observed for CMP in the mixed solvent systems used in these experiments. In all of the solvent systems studied, CMP has an apparent isosbestic point near 280 nm. For poly(C), however, the absorbance at 280 nm increases with temperature. Presumably the optical changes associated with solvent binding to cytosine residues in the polymer are similar to those observed for CMP. Therefore, the temperature-dependent absorbance for poly(C) at 280 nm can be attributed to base stacking.

Equilibrium Thermodynamics. Absorbance vs. temperature profiles for poly(C) in various aqueous solvent mixtures were fit to

$$\epsilon = \alpha(\epsilon_s - \epsilon_u) + \epsilon_u \quad (1)$$

where ϵ is the observed extinction coefficient of the polymer, ϵ_s and ϵ_u are the extinctions of the fully stacked (helical) and unstacked (coil) states, respectively, and α is the fraction of molecules in the stacked state

$$\alpha = \frac{K}{1+K} = \frac{\exp(-\Delta H/RT + \Delta S/R)}{1 + \exp(-\Delta H/RT + \Delta S/R)} \quad (2)$$

where K, ΔH, and ΔS are the equilibrium constant, enthalpy, and entropy, respectively, for the coil to helix process. A nonlinear least-squares program was used to obtain ϵ_s, ϵ_u, ΔH, and ΔS (Dewey & Turner, 1979). The measured extinctions, ϵ, can then be converted to α's by using eq 1 and the fitted values of ϵ_s and ϵ_u. The resulting fraction of molecules in the coiled state, $1 - \alpha$, is plotted vs. temperature in Figure 1. The limiting absorbances used to generate these curves are listed in Table I and allow reconstruction of the original experimental curves. In contrast to melting curves of double-stranded RNA (Chamberlin & Patterson, 1965), these curves are very broad. No more than 80% of the transition occurs between 0 and 90 °C. The effect of cosolvents on the stability of the helix is similar to that observed for double-stranded DNA (Herskovits, 1962); 1 M salt stabilizes the helix and all other cosolvents lower the transition temperature.

The thermodynamics derived from fitting the data are listed in Table II. For each solvent, the reported parameters and estimated errors are the average values and standard deviations, respectively, of parameters obtained from fits to this two-state model of at least three experimental melting curves. The standard deviation in K was <10% for all solvents. The enthalpy of −8.6 ± 0.8 kcal/mol for the coil to helix transition of poly(C) in 0.05 M sodium cacodylate, pH 7.0, agrees with previous spectroscopic measurements at higher ionic strength (Pörschke, 1976; Brahms et al., 1967).

Table I: Absorbances of Fully Helical and Fully Coiled States of Poly(C) Samples Used for Figure 1[a]

solvent[b]	$A_{helical}$	A_{coil}
H_2O	0.83	1.47
1 M NaCl	0.51	0.91
5 mol % EtOH	0.52	0.97
10 mol % EtOH	0.87	1.43
5 mol % formamide	1.16	1.86
5 mol % urea	0.73	1.14
5 mol % CH_3CN	1.11	1.84
10 mol % glycerol	0.70	1.12
15 mol % glycerol	0.90	1.35
2.9 mol % sucrose	0.55	0.92

[a] Two-state model. [b] All solvents contain 0.05 M sodium cacodylate, pH 7.0.

Table II: Thermodynamic Parameters for Coil to Helix Transition of Poly(C) in 0.05 M Sodium Cacodylate, pH 7.0[a]

	two-state model, $\sigma = 1$		Ising model, $\sigma = 0.25$	
solvent[b]	$-\Delta H$ (kcal/mol)	$-\Delta S$ (eu)	$-\Delta H_i$ (kcal/mol)	$-\Delta S_i$ (eu)
H_2O	8.6 ± 0.8	26.7 ± 2.7	3.8 ± 0.2	11.9 ± 0.9
0.2 M NaCl[c]	9.0 ± 0.3	27.6 ± 1.0	4.1 ± 0.1	12.6 ± 0.5
1 M NaCl	9.4 ± 0.7	28.4 ± 2.6	4.4 ± 0.2	13.4 ± 0.9
5 mol % EtOH	8.8 ± 0.9	28.4 ± 3.4	4.0 ± 0.5	12.8 ± 1.4
10 mol % EtOH	8.7 ± 0.8	27.9 ± 2.6	3.8 ± 0.4	12.4 ± 1.2
10 mol % PrOH	11.7 ± 0.4	37.4 ± 1.1	5.3 ± 0.2	17.2 ± 0.6
5 mol % formamide	7.4 ± 1.0	23.7 ± 3.5	3.3 ± 0.5	10.5 ± 1.6
5 mol % urea	7.5 ± 0.9	23.7 ± 3.1	3.3 ± 0.4	10.5 ± 1.4
5 mol % CH_3CN	7.9 ± 0.5	25.1 ± 1.8	3.5 ± 0.2	11.2 ± 0.8
10 mol % glycerol	9.0 ± 0.5	29.3 ± 1.5	3.9 ± 0.2	12.7 ± 0.6
15 mol % glycerol	8.7 ± 0.7	28.9 ± 2.5	3.9 ± 0.4	13.0 ± 1.4
2.9 mol % sucrose	7.8 ± 1.1	24.3 ± 3.6	3.7 ± 0.4	11.4 ± 1.3

[a] Two-state model and Ising model with $\sigma = 0.25$. [b] All solvents except 0.2 M NaCl contain 0.05 M sodium cacodylate, pH 7.0. [c] 0.01 M sodium phosphate, 0.001 M EDTA, and 0.2 M NaCl, pH 7.0.

An accurate determination of the equilibrium constant is necessary to obtain rate constants from relaxation times for unimolecular reactions. It is therefore essential to critically evaluate the method used to obtain these thermodynamic parameters.

One effect that could distort the thermodynamics is temperature-dependent extinctions, ϵ_s and ϵ_u. The temperature dependence of the absorbance of CMP is a good estimate for the temperature dependence of ϵ_u. Under conditions identical with those used for poly(C) melting curves, the absorbance of 5′-CMP between 0 and 88 °C decreases between 2 and 5% in all the solvents except 10% ethanol where the decrease was 7%. This confirms compensation of the temperature-dependent extinction by volume expansion, as discussed above. It has previously been shown that the fitting program will give reliable results if the temperature dependence of the extinctions is <5% from 5 to 70 °C (Dewey & Turner, 1979). Thus this should not be a problem with poly(C).

Another potential problem in determining the thermodynamics is the ability of poly(C) to form double-helical structures. This is known to occur at pH 4 but not at pH 7 in

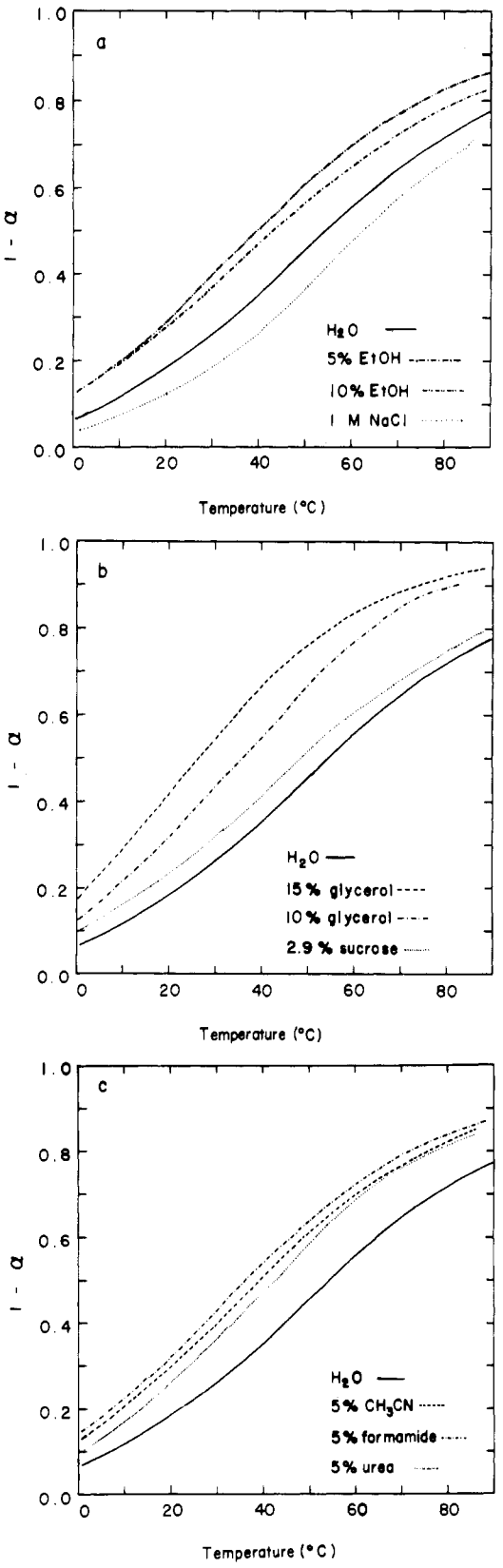

FIGURE 1: Fraction of molecules in coiled state as a function of temperature for poly(C) in 0.05 M sodium cacodylate, pH 7.0. The fraction of molecules in the coiled state was calculated from the measured absorbance according to eq 1. Values of ϵ_s and ϵ_u were obtained from a nonlinear least-squares fit of the data to a two-state model. The curves in this figure can be converted to absorbance vs. temperature plots by using eq 1 and the values of A_u and A_s in Table I. (a) (—) H_2O; (-·-) 5 mol % ethanol; (-··-) 10 mol % ethanol; (···) 1 M NaCl. (b) (—) H_2O; (- - -) 15 mol % glycerol; (-·-) 10 mol % glycerol; (···) 2.9 mol % sucrose. (c) (—) H_2O; (- - -) 5 mol % acetonitrile; (-·-) 5 mol % formamide; (···) 5 mol % urea.

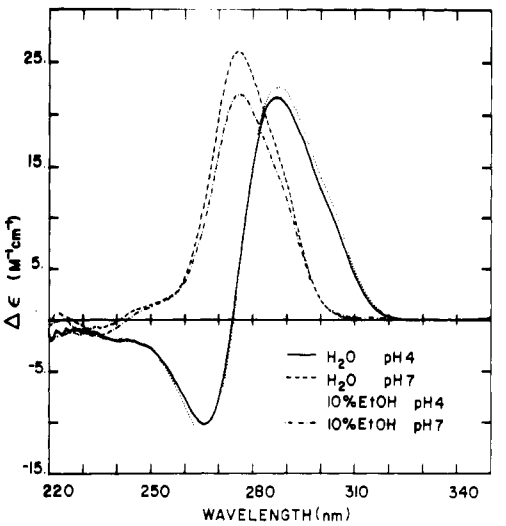

FIGURE 2: Circular dichroism spectra of poly(C) at 2 °C in 0.05 M sodium acetate (pH 4.0) or 0.05 M sodium cacodylate (pH 7.0). (—) Aqueous buffer, pH 4.0; (- - -) aqueous buffer, pH 7.0; (···) 10 mol % ethanol, pH 4.0; (-·-) 10 mol % ethanol, pH 7.0. Spectral band-pass = 1 nm. For calculation of $\Delta\epsilon$ from the ellipticity, it was assumed ϵ was independent of solvent (see text).

aqueous buffer [Guschlbauer (1975) and references cited therein]. It is possible the cosolvents used in this study could stabilize the double-helical species at pH 7 and thereby distort the melting curves in Figure 1. Fortunately, CD spectra of the poly(C) double helix and single strand are quite different (Brahms et al., 1967). Figure 2 shows the CD spectra for poly(C) at pH 4 and 7 in aqueous buffer and 10 mol % ethanol. If poly(C) in 10 mol % ethanol at pH 7 formed some double-helical structures, the maximum at 276 nm would shift to longer wavelengths, and the ellipticity above 300 nm would increase relative to that observed for the aqueous solution. Instead, the spectra for the two solvents are similar at each pH, indicating the same species are present. Similar CD spectra were obtained for poly(C) at pH 4 and 7 in 5 mol % urea, 5 mol % acetonitrile, and 10 mol % glycerol. Thus the CD spectra indicate no double-helical poly(C) in these solvent mixtures at pH 7.

Another criterion that can be used to eliminate the possibility of double-helical structures is the shape of the melting curves in Figure 1. The melting transition for double-stranded poly(C) is quite sharp (Akinrimisi et al., 1963). In aqueous buffer with 0.05 M sodium acetate, pH 4, we observe 20% hypochromicity between 70 and 84 °C. Similar absorbance increases are observed in the solvent mixtures at pH 4. [Above the T_m, however, we observe an irreversible absorbance decrease that may be due to deamination of cytosine (Shapiro & Klein, 1966).] If double-helical poly(C) were present at pH 7, a sharp absorbance increase would be observed in the melting curves. This is not seen in Figure 1. Computer-generated curves indicated it would be clearly visible if only 5% of the poly(C) were double stranded. Moreover, when curves generated by assuming <5% double helix were analyzed, the fitting program converged to within 10% of the single-strand ΔH and ΔS used to generate the curves. Thus, it appears that double-helical species are not affecting the derived thermodynamics.

Perhaps the largest uncertainty in deriving thermodynamics from poly(C) melting curves results from the choice of analytical model. Thus, if the coil to helix transition of poly(C) were cooperative, the one-dimensional Ising model would be more appropriate than the two-state model for analysis of absorbance vs. temperature data (Zimm & Bragg, 1959;

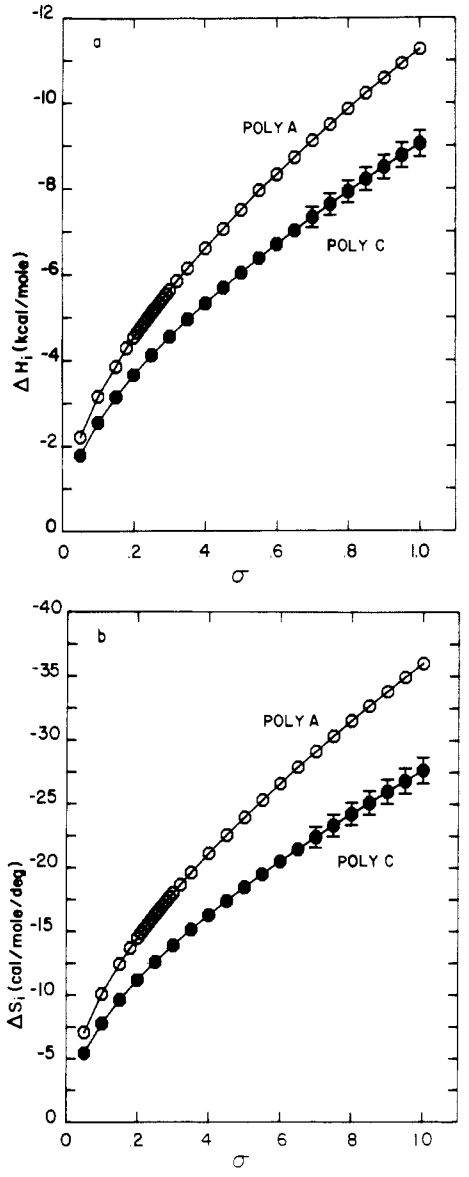

FIGURE 3: Enthalpy and entropy of coil to helix transition obtained from a fit of melting curves to Ising model for a fixed value of σ plotted vs. σ. (○) Poly(A) in 0.05 M sodium cacodylate, pH 7.0; (●) poly(C) in 0.01 M sodium phosphate, 0.001 M EDTA, and 0.2 M NaCl, pH 7.0. A similar curve for poly(C) in 0.05 M sodium cacodylate, pH 7.0, is in the supplementary material.

Applequist, 1963). To investigate the applicability of the Ising model, we fit experimental melting curves by using

$$\alpha = 0.5 + 0.5(s - 1)[(1 - s)^2 + 4\sigma s]^{-1/2} \quad (3a)$$

$$s = \exp(-\Delta H_i/RT + \Delta S_i/R) \quad (3b)$$

Here s, ΔH_i, and ΔS_i are the equilibrium constant, enthalpy, and entropy, respectively, for adding one base to the end of a helical segment, and σ is the cooperativity parameter. For a fixed value of σ, a nonlinear least-squares fit to eq 1 was used to obtain ΔH_i, ΔS_i, ϵ_u, and ϵ_s. Good fits were obtained for all values of σ between 0.05 and 1.0. Similar results were obtained from fitting previously reported melting curves for poly(A) in 0.05 M sodium cacodylate, pH 7 (Dewey & Turner, 1979). Evidently, the spectroscopic data alone cannot be used to determine the cooperativity. The enthalpies and entropies obtained as a function of σ are plotted in Figure 3 for poly(C) in 0.01 M phosphate, 0.001 M EDTA, and 0.2 M NaCl, pH 7, and for poly(A) in 0.05 M cacodylate, pH 7. Curves for poly(C) in 0.05 M cacodylate are available in the microfilm edition (see paragraph at end of paper regarding supplementary material). Unfortunately, the derived thermodynamics are very sensitive to σ.

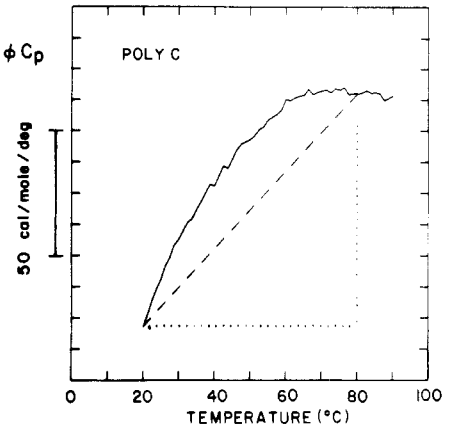

FIGURE 4: Excess heat capacity plotted vs. temperature for poly(C) in 0.01 M sodium phosphate, 0.001 M EDTA, and 0.2 M NaCl, pH 7.0. The scale on the oridinate is 12.5 cal/(mol deg) per division. The curve is an average of five scans of poly(C) samples ranging in concentration from 11 to 24 mM. The average of four buffer vs. buffer runs was subtracted from the experimental curve. The dashed line is drawn between the excess heat capacities at 20 and 80 °C. The area between this line and the heat capacity curve is 1.2 kcal/mol. The area between the dotted line and the heat capacity curve is 4.0 kcal/mol.

The above results emphasize the importance of determining the cooperativity parameter, σ. In principle, σ can be deduced from the chain length dependence of hypochromicity, if end effects are negligible. However, for σ's of 0.1–1, hypochromicity differences will be significant only for chain lengths of about 2–7, where end effects are likely to be important. Thus, optical measurements alone are not likely to yield reliable cooperativity parameters.

An alternative for deriving σ is to combine spectroscopic and calorimetric data. Excess heat capacity (ϕC_p) measured by differential scanning calorimetry of poly(C) in 0.01 M phosphate, 0.001 M EDTA, and 0.2 M NaCl, pH 7, is plotted vs. temperature in Figure 4. The salt concentration was chosen to minimize problems associated with potential imbalances in ionic strength between sample and reference cells. Such imbalances can arise from Donnan equilibria. For comparison, an excess heat capacity curve can also be derived from the spectroscopic data by using

$$\phi C_p = \Delta H \frac{d\alpha}{dT} \quad (4)$$

This curve will depend on the σ assumed. Agreement between the spectroscopic and calorimetric excess heat capacity curves can therefore be used to determine σ. Unfortunately, there are several problems in making this comparison. Firstly, the DSC experiment does not give an absolute value of the excess heat capacity. Secondly, the DSC experiment may contain heat capacity contributions from processes not associated with single-strand stacking. However, if this background heat capacity is a linear function of temperature, then the curvature of the heat capacity curve will reflect single-strand stacking. The easiest way to use this curvature is to draw a straight line between the excess heat capacities at two temperatures and integrate the area of the curve above this line (see dashed line in Figure 4). Integration of five DSC scans of poly(C) between 20 and 80 °C gave an area of 1.2 ± 0.2 kcal/mol. This area can then be compared with similar areas obtained from heat capacity curves derived from spectroscopic results. For example, Figure 5 shows the curve generated by eq 4 when σ = 1.0, ΔH_i = −9.04 kcal/mol of stack, and ΔS_i = −27.6

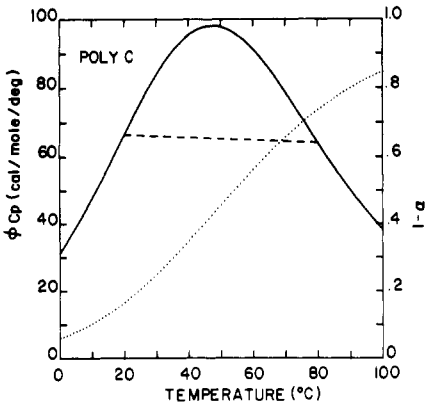

FIGURE 5: Calculated heat capacity curve for coil to helix transition of poly(C) in 0.01 M sodium phosphate, 0.001 M EDTA, and 0.2 M NaCl, pH 7.0. $\Delta H = -9.04$ kcal/mol; $\Delta S = -27.6$ cal/(mol deg); $\sigma = 1.0$. The solid line is the excess heat capacity; the dotted line is the fraction of bases in the coil conformation. The dashed line was drawn from 20 to 80 °C. The area between that line and the heat capacity curve is 1.24 kcal/mol.

cal/(mol deg). The ΔH_i and ΔS_i are those derived from fitting poly(C) melting curves in calorimetry buffer assuming $\sigma = 1.0$ (see Figure 3). The area enclosed by a line drawn between the excess heat capacities at 20 and 80 °C (the dashed line in Figure 5) is 1.24 kcal/mol, in excellent agreement with the calorimetric value of 1.2 kcal/mol. For a σ of 0.5, the area is only 0.79 kcal/mol. Thus, comparison of spectroscopic and calorimetric results for poly(C) indicates σ is 1.0 ± 0.2 and ΔH_i is −9.0 ± 1.5 kcal/mol of stack. Similar values of σ and ΔH_i are obtained if the integration is performed between 25 and 80 °C or 20 and 75 °C.

A more sophisticated analysis can be made by comparing the shapes of the calorimetric and spectrophotometric curves. If all contributions to the calorimetric ϕC_p curve that are not associated with single-strand stacking are linear with temperature, then the experimental curve can be fit to

$$\phi C_p = \Delta H \frac{d\alpha}{dT} + b + mT \qquad (4a)$$

where b and m are the intercept and slope, respectively, of the background heat capacity. For fixed values of σ, ΔH, and ΔS derived from the spectroscopic data (see Figure 3), the difference between the calorimetric ϕC_p and the spectroscopically predicted ϕC_p (eq 4) as a function of temperature can be fit by a linear least-squares algorithm. The standard deviation in the fit is sensitive to σ and is minimized when σ is between 0.9 and 1.0. The curve calculated from eq 4a by using the b and m values fitted when $\sigma = 1.0$ is shown in Figure 6, along with the experimental calorimetric points.

The above treatment assumes the curvature in the heat capacity and optical melting curves is due only to the single-strand stacking reaction. To test this assumption for calorimetry, we ran DSC scans with cytidine and CMP in the 0.2 M NaCl buffer. The heat capacity vs. temperature curves were linear with a positive slope. Thus, the upward slope of the heat capacity curve apparent in Figures 4 and 6 may be due to solvent interaction with the bases and/or ionic interactions. Similar base lines have been observed in DSC measurements on poly(A) (Suurkuusk et al., 1977; Filimonov & Privalov, 1978). As long as this background heat capacity is a linear function of temperature, calorimetric and spectroscopic data can be combined to obtain σ.

The method described above was devised to give an experimental estimate of the cooperativity parameter as well as ΔH. An alternative way to derive ΔH is to integrate the area

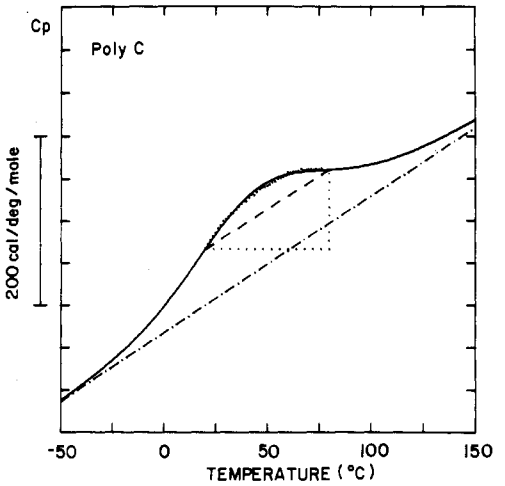

FIGURE 6: Experimental and calculated heat capacity curves for coil to helix transition of poly(C). $\Delta H = -9.04$ kcal/mol; $\Delta S = -27.6$ cal/(mol deg); $\sigma = 1.0$. The solid curve (—) is the sum of the excess heat capacity curve in Figure 5 and a linear background heat capacity (–·–). The experimental data are represented as the dots superimposed on the solid curve. The scale on the ordinate is 50 cal/(mol deg) per division. The dashed and dotted lines correspond to those in Figure 4.

Table III: Relaxation Times and Rate Constants for Coil to Helix Transition of Poly(C) in 0.05 M Sodium Cacodylate, pH 7, at 30 °C

solvent[a]	τ (ns)	$k_1 \times 10^{-6}$ (s^{-1})	$k_{-1} \times 10^{-6}$ (s^{-1})
H_2O	40 ± 8	17 ± 4 (41)[b]	8 ± 2 (28)[b]
1 M NaCl	49 ± 8	15 ± 3 (31)	4.5 ± 0.8 (18)
5 mol % EtOH	40 ± 9	15 ± 3 (39)	9.9 ± 2.3 (35)
10 mol % EtOH	56 ± 10	10 ± 2 (28)	8 ± 1 (25)
10 mol % PrOH	56 ± 6	10 ± 1 (29)	7 ± 1 (25)
5 mol % formamide	36 ± 6	16 ± 3 (44)	12 ± 2 (39)
5 mol % urea	45 ± 10	14 ± 3 (36)	9 ± 2 (29)
5 mol % CH_3CN	32 ± 6	18 ± 4 (50)	13 ± 3 (42)
10 mol % glycerol	90 ± 18	6 ± 1 (18)	5 ± 1 (16)
15 mol % glycerol	195 ± 35	2.3 ± 0.4 (7)	2.8 ± 0.5 (8)
2.9 mol % sucrose	106 ± 10	6.2 ± 0.6 (15)	3.2 ± 0.3 (11)

[a] All solvents contain 0.05 M sodium cacodylate, pH 7.0. [b] The rates inside the parentheses are calculated according to the kinetic Ising model with $\sigma = 0.25$. The rates outide the parentheses are for the two-state model.

under the heat capacity curve shown in Figure 4 and then divide by the fraction of the transition that occurs over the measured temperature range. This fraction can be derived from the optical data, and for poly(C) it is relatively independent of σ. For example, the fraction of the transition occurring between 20 and 80 °C is 0.57 for $\sigma = 1$ and 0.52 for $\sigma = 0.3$. The integrated area of the heat capacity curve from 20 to 80 °C is 4.0 kcal/mol. (This area is outlined by the dotted lines in Figures 4 and 6.) If $\sigma = 1$, this corresponds to a total ΔH of −7.0 kcal/mol for the coil to helix transition. This treatment requires different assumptions than the one described previously. In particular, it assumes the excess heat capacity due to single-strand stacking is 0 cal/(mol deg) at 20 °C and that all the excess heat capacity above 20 °C is due to the coil to helix transition.

Kinetics. The relaxation times at 280 nm for poly(C) at 30 °C in mixed aqueous solvents are listed in Table III. A typical relaxation is shown in Figure 7. The rapid initial rise corresponds to the heating time of ~20 ns (Dewey & Turner, 1978) and is observed in aqueous solutions of CMP. It is most likely due to the temperature-dependent binding of solvent to cytosine residues. Although 280 nm is near the isosbestic point for this reaction, the 16-nm band-pass of the monochromator

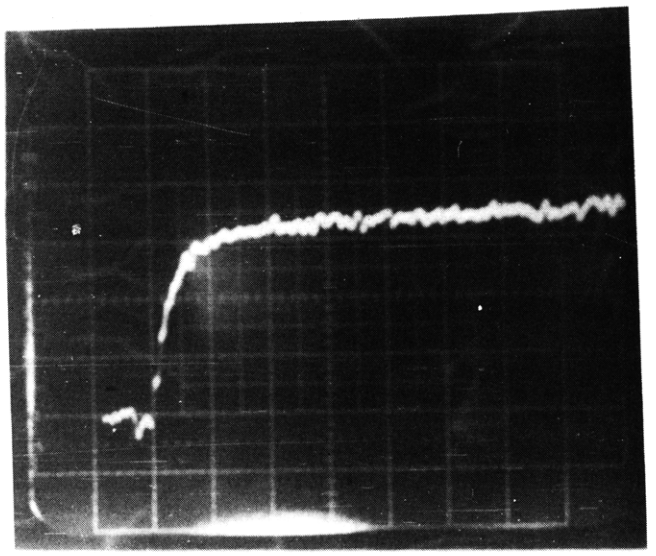

FIGURE 7: Relaxation observed at 280 nm for poly(C) at 30 °C in 0.05 M sodium cacodylate, pH 7.0. Horizontal scale is 50 ns/major division.

Table IV: Relaxation Times, Rate Constants, and Activation Parameters for Coil to Helix Transition of Poly(C) in 0.05 M Sodium Cacodylate, pH 7.0[a]

		τ (ns)	$k_1 \times 10^{-6}$ (s^{-1})	$k_{-1} \times 10^{-6}$ (s^{-1})
H_2O	T (°C):			
	10	45 ± 7	19 ± 3 (34)	3.1 ± 0.6 (15)
	20	39 ± 9	20 ± 5 (42)	5.5 ± 1.3 (23)
	30	40 ± 8	17 ± 4 (41)	7.6 ± 1.6 (28)
	40	34 ± 7	17 ± 4 (48)	12.1 ± 2.3 (35)
	E_a (kcal/mol)		−0.8 (1.8)	7.8 (4.9)
	$\Delta S^{\ddagger}$ (eu)		−30 (−20)	−2 (−10)
1 M NaCl	T (°C):			
	15	67 ± 13	13 ± 3 (22)	1.8 ± 0.4 (7)
	20	58 ± 11	15 ± 3 (26)	2.6 ± 0.5 (12)
	30	49 ± 8	15 ± 3 (31)	4.5 ± 0.8 (18)
	40	38 ± 8	18 ± 4 (43)	8.6 ± 1.7 (31)
	E_a (kcal/mol)		1.9 (4.7)	11.1 (9.9)
	$\Delta S^{\ddagger}$ (eu)		−22 (−11)	6 (6)
5 mol % EtOH	T (°C):			
	10	118 ± 51	7 ± 3 (14)	1.6 ± 0.7 (8)
	20	57 ± 9	13 ± 2 (29)	5.1 ± 0.9 (20)
	30	40 ± 9	15 ± 3 (39)	9.9 ± 2.3 (35)
	40	34 ± 7	14 ± 3 (42)	15.2 ± 3.4 (46)
	E_a (kcal/mol)		4.2 (6.6)	13.2 (10.6)
	$\Delta S^{\ddagger}$ (eu)		−14 (−4)	15 (9)
10 mol % EtOH	T (°C):			
	10	131 ± 31	6 ± 1 (12)	1.6 ± 0.4 (7)
	20	100 ± 16	7 ± 1 (16)	3.1 ± 0.6 (12)
	30	56 ± 10	10 ± 2 (28)	7.6 ± 1.4 (25)
	40	44 ± 12	11 ± 3 (33)	12.3 ± 3.6 (36)
	E_a (kcal/mol)		3.7 (6.2)	12 (10)
	$\Delta S^{\ddagger}$ (eu)		−16 (−6)	12 (6)

[a] Two-state and kinetic Ising model with $\sigma = 0.25$ (in parentheses).

does not permit total discrimination against this signal. To eliminate it, we ignored the first 20 ns of the traces in evaluating the relaxation times. The slower exponential rise is not observed in solutions of CMP and is due to the helix to coil transition in poly(C).

The relaxation time is independent of poly(C) concentration between 3 and 20 mM indicating a unimolecular reaction is being observed. For poly(C) in 0.05 M sodium cacodylate, pH 7, the relaxation times at 260, 275, and 280 nm were

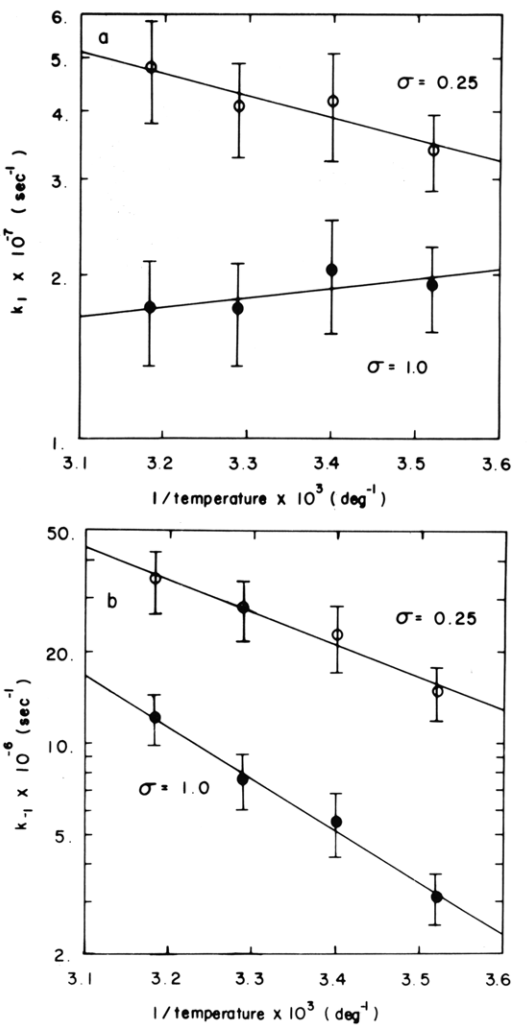

FIGURE 8: Eyring plot for coil to helix transition of poly(C) in 0.05 M sodium cacodylate, pH 7.0; (●) two-state model ($\sigma = 1$) and (○) kinetic Ising model with $\sigma = 0.25$.

identical within experimental error. This wavelength independence suggests a simple two-state reaction is being observed.

The kinetic results were analyzed with the two-state model. The relaxation time is given by

$$1/\tau = k_1 + k_{-1} \quad (5)$$

where k_1 is the rate of helix formation and k_{-1} is the rate of coil formation. The two-state thermodynamic parameters listed in Table I were used to calculate an equilibrium constant to partition the relaxation time into forward and reverse rates.

The kinetic Ising model (Schwarz, 1965, 1972; Dewey & Turner, 1979) was also used to analyze the data. The value of the cooperativity parameter, σ, was fixed at 0.25, and the Ising model thermodynamic parameters in Table II were used to calculate $s = k_1/k_{-1}$, the equilibrium constant for stacking a base on a helical segment. The rates calculated by using the two-state model and the kinetic Ising model are reported in Table III. The rates in 1 M NaCl agree well with those obtained previously by using the cable temperature-jump technique (Pörschke, 1976).

The Eyring equation (eq 6) was used to obtain activation

$$k = (eRT/hN) \exp(\Delta S^{\ddagger}/R) \exp(-E_a/RT) \quad (6)$$

energies, E_a, and entropies, $\Delta S^{\ddagger}$, at 30 °C. They are listed in Table IV. The estimated errors in these parameters are 1 kcal/mol for E_a and 3 eu for $\Delta S^{\ddagger}$. The Eyring plots for

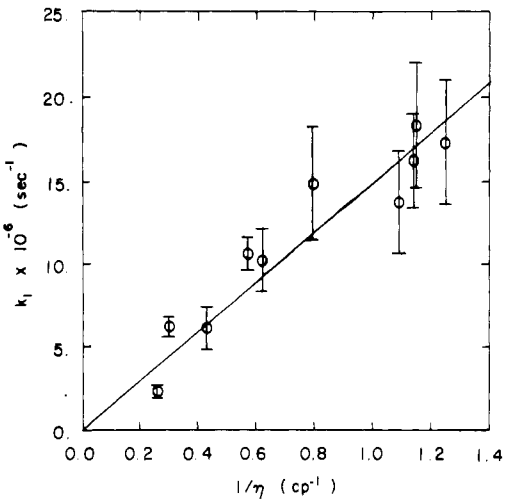

FIGURE 9: Plot of rate of helix formation vs. reciprocal solvent viscosity for poly(C) in 0.05 M sodium cacodylate, pH 7.0, 30 °C. Two-state model.

poly(C) in 0.05 M sodium cacodylate, pH 7, are shown in Figure 8.

The most obvious trend in the rate constants in Table III is the correlation of forward rate with reciprocal solvent viscosity. The two-state forward rates are plotted vs. reciprocal viscosity in Figure 9. A similar plot is generated if rate constants from the kinetic Ising model are used.

The reverse rates are influenced less by solvent than the forward rates. Ethanol and propanol have no effect on the rate of coil formation at 30 °C; formamide and acetonitrile increase the reverse rate slightly, and high-viscosity cosolvents like glycerol or sucrose slow down the reverse rate.

Discussion

One important finding of this work is that spectroscopic and calorimetric data can be combined to give values of the cooperativity parameter, σ, for single-strand stacking in poly(C). Due to the broad nature of the transition, neither technique alone can be used to determine the enthalpy. Comparison of results of the two methods, however, indicates that σ is between 0.8 and 1.0, suggesting single-strand stacking in poly(C) is almost noncooperative. These values of σ correspond to a ΔH between −7.5 and −9.0 kcal/mol of stack. The conclusion that poly(C) stacking is nearly noncooperative agrees with earlier spectroscopic measurements on oligocytidylates (Brahms et al., 1967; Adler et al., 1967).

The method described above for obtaining the cooperativity parameter can also be used for poly(A). Two measurements of excess heat capacity as a function of temperature have been reported for poly(A) stacking (Suurkuusk et al., 1977; Filimonov & Privalov, 1978). Integration of the raw data from these papers between 10 and 70 °C in the manner described above results in areas of 2.0 (Suurkuusk et al., 1977) and 1.3 kcal/mol (Filimonov & Privalov, 1978). As outlined for poly(C), the spectroscopic data for poly(A) presented in Figure 3 can be combined with the calorimetric data to obtain σ and ΔH. An area of 2.0 kcal/mol between 10 and 70 °C corresponds to $\sigma = 0.6$ and $\Delta H_i = -8.0$ kcal/mol of stack; an area of 1.3 kcal/mol corresponds to $\sigma = 0.3$ and $\Delta H_i = -5.6$ kcal/mol of stack. The calorimetric results were obtained at 0.1–0.2 M ionic strength, and the spectroscopic results were obtained at 0.05 M. However, the calorimetric results are reported to be insensitive to ionic strength from 0.01 to 0.1 M (Filimonov & Privalov, 1978). The discrepancy between the cooperativity parameters obtained by analysis of these two heat capacity curves suggests additional calorimetric experiments are necessary before σ can be accurately determined for poly(A).

The cooperativity parameters determined for poly(C) and poly(A) range from 0.3 to 1. The rate constants for poly(C) listed in Table III were derived by assuming $\sigma = 1$ or $\sigma = 0.25$. The calorimetric data indicate 0.25 is well below the true value of σ for poly(C). Nevertheless, the qualitative trends in the rates with solvent composition are the same for both values of σ. In analyzing these trends, we have assumed σ is independent of solvent. A direct test of this assumption requires calorimetric experiments on the solvent mixtures. This is an extremely difficult task for such a broad transition. However, there are theoretical considerations that support the assumption. In particular, the small cooperativity can be attributed to the fact that helix initiation requires restriction of rotation around one more bond than helix propagation (Applequist & Damle, 1966). For example, if this restriction reduces the number of configurations about this bond by a factor of 2, σ is predicted to be 0.5 (Applequist & Damle, 1966). This entropy term should not be solvent dependent. Thus, it seems reasonable to assume that σ is solvent independent.

The clearest correlation discovered in this study is that the forward rate for poly(C) stacking depends on reciprocal solvent viscosity (see Figure 9). This suggests stacking is a diffusion-controlled reaction. The low activation energy supports this. However, the absolute magnitude of the forward rate, about 2×10^7–4×10^7 s^{-1}, is slower than expected for diffusion control. For example, the bimolecular rate for monomer stacking of adenine derivatives and simple dye molecules is on the order of 10^9 M^{-1} s^{-1} (Pörschke & Eggers, 1972; Garland & Patel, 1974; Dewey et al., 1978, 1979). Considering the high local concentration of cytosine along the polymer backbone, the unimolecular rate for poly(C) should be at least as large. The relatively slow forward rate is associated with an unfavorable activation entropy barrier to helix formation. The magnitude of this barrier is consistent with a conformationally restricted transition state in which most or all six of the backbone bonds must be in a particular conformation. Diffusion across a single rotational barrier then results in helix formation. Similar observations and interpretations have been made for poly(A) stacking (Dewey & Turner, 1979, 1980). The forward rate for poly(C) is 1.5–3-fold faster than that of poly(A). Cytosine is smaller than adenine and therefore should diffuse faster, supporting the proposed mechanism.

The effects of solvent on the poly(C) reverse rates are less straightforward than for the forward rate. The high viscosity cosolvents, glycerol and sucrose, decrease the reverse rate, suggesting it is at least partially controlled by rotational diffusion. Formamide and acetonitrile at 5 mol % increase the rate by ~50% relative to water. This may indicate these molecules attack a cytosine stack more effectively than water. Increasing the NaCl concentration from 0 to 1 M almost halves the reverse rate. Presumably, this reflects greater shielding of the negative charges along the backbone.

The work discussed above provides some insights into the forces stabilizing helical structures in nucleic acids. The two different methods for analyzing the calorimetric data give stacking enthalpies of −7 and −9 kcal/mol of stack for poly(C). These enthalpies provide an estimate for the contribution of single-strand stacking to double-helix formation, if adjustments are made for stacking present before the double helix is formed. Thus the enthalpy associated with poly(C) becoming fully stacked at 54 °C is between −3.5 and −4.6 kcal/mol of stack. These should be an upper limit for the single-strand stacking contribution to double-helix formation because the double-

helical geometry may restrict the bases to less favorable orientations for stacking. For comparison, the enthalpy for forming a poly(I)–poly(C) double helix from separated strands at 54 °C is −6.5 kcal/mol of base pairs (Hinz et al., 1970). If the assumption is made that at low ionic strength, poly(I) stacking has no significant enthalpy change (Hinz et al., 1970), then it follows that single-stranded stacking accounts for more than half of the enthalpy associated with double-helix formation.

The kinetic results indicate the enthalpy of single-strand stacking is due to the activation energy of the reverse rate. This is consistent with the common concept that "stacking" interactions between bases dominate the thermodynamics. The kinetics also indicate this stacking interaction is greater for adenine than cytosine, even though poly(C) has a higher transition temperature. Thus, the helix to coil rate is faster for poly(C) than for poly(A), and its activation energy is lower. The higher equilibrium constant for poly(C) stacking appears to be due to the smaller size of cytosine which results in a faster diffusion-controlled forward rate. Finally, the reverse rates in various solvents provide no evidence for a surface tension dependence that might be expected if solvent cavity forces were important in determining stability (Sinanoğlu & Abdulnur, 1965; Sinanoğlu, 1968). If cavity forces were important, the lifetime of the stacked state should be very sensitive to surface tension. The surface tensions of H_2O, 10 mol % ethanol, and 10 mol % propanol are respectively 71, 35, and 26 dyn/cm at 30 °C; the respective lifetimes of the stacked states are 125 ± 30, 125 ± 16, and 143 ± 20 ns.

Supplementary Material Available

Two figures showing plots of ΔH and ΔS vs. σ for poly(C) in 0.05 M sodium cacodylate, pH 7 (2 pages). Ordering information is given on any current masthead page.

References

Adler, A., Grossman, L., & Fasman, G. D. (1967) *Proc. Natl. Acad. Sci. U.S.A. 57*, 423–430.

Akinrimisi, E. O., Sander, C., & Ts'o, P. O. P. (1963) *Biochemistry 2*, 340–344.

Albergo, D. D., Marky, L. A., Breslauer, K. J., & Turner, D. H. (1981) *Biochemistry* (first of three papers in this issue).

Applequist, J. (1963) *J. Chem. Phys. 38*, 934–941.

Applequist, J., & Damle, V. (1966) *J. Am. Chem. Soc. 88*, 3895–3900.

Arnott, S., Chandrasekaran, R., & Leslie, A. G. W. (1976) *J. Mol. Biol. 106*, 735–748.

Brahms, J., Maurizot, J. C., & Michelson, A. M. (1967) *J. Mol. Biol. 25*, 465–480.

Cantor, C. R., & Schimmel, P. R. (1980) *Biophysical Chemistry Part I: The Conformation of Biological Macromolecules*, Chapter 6, W. H. Freeman, San Francisco, CA.

Casey, J., & Davidson, N. (1977) *Nucleic Acids Res. 4*, 1539–1552.

Chamberlin, M. J., & Patterson, D. L. (1965) *J. Mol. Biol. 12*, 410–428.

Crothers, D. M., & Zimm, B. H. (1964) *J. Mol. Biol. 9*, 1–9.

DeWachter, R., & Fiers, W. (1971) *Methods Enzymol. 21*, 167–187.

Dewey, T. G., & Turner, D. H. (1978) *Adv. Mol. Relaxation Interact. Processes 13*, 331–350.

Dewey, T. G., & Turner, D. H. (1979) *Biochemistry 18*, 5757–5762.

Dewey, T. G., & Turner, D. H. (1980) *Biochemistry 19*, 1681–1685.

Dewey, T. G., Wilson, P. S., & Turner, D. H. (1978) *J. Am. Chem. Soc. 100*, 4550–4554.

Dewey, T. G., Raymond, D. A., & Turner, D. H. (1979) *J. Am. Chem. Soc. 101*, 5822–5826.

Felsenfeld, G., & Miles, H. T. (1967) *Annu. Rev. Biochem. 36*, 407–448.

Filimonov, V. V., & Privalov, P. L. (1978) *J. Mol. Biol. 122*, 465–470.

Garland, F., & Patel, R. C. (1974) *J. Phys. Chem. 78*, 848–850.

Guschlbauer, W. (1975) *Nucleic Acids Res. 2*, 353–360.

Herskovits, T. T. (1962) *Arch. Biochem. Biophys. 97*, 474–484.

Hinz, H.-J., Haar, W., & Ackermann, Th. (1970) *Biopolymers 9*, 923–936.

Johnson, W. C., Jr., Vipond, P. M., & Girod, J. C. (1971) *Biopolymers 10*, 923–933.

Lawaczeck, R., & Wagner, K. G. (1974) *Biopolymers 13*, 2003–2014.

Pörschke, D. (1973) *Eur. J. Biochem. 39*, 117–126.

Pörschke, D. (1976) *Biochemistry 15*, 1495–1499.

Pörschke, D. (1978) *Biopolymers 17*, 315–323.

Pörschke, D., & Eggers, F. (1972) *Eur. J. Biochem. 26*, 490–498.

Pullman, A., & Pullman, B. (1968) *Adv. Quantum Chem. 4*, 267–325.

Pullman, B., & Pullman, A. (1969) *Prog. Nucleic Acid Res. Mol. Biol. 9*, 327–402.

Schwarz, G. (1965) *J. Mol. Biol. 11*, 64–77.

Schwarz, G. (1972) *J. Theor. Biol. 36*, 569–580.

Shapiro, R., & Klein, R. S. (1966) *Biochemistry 5*, 2358–2362.

Sinanoğlu, O. (1968) *Mol. Assoc. Biol., Proc. Int. Symp., 1967*, 427–445.

Sinanoğlu, O., & Abdulnur, S. (1965) *Fed. Proc., Fed. Am. Soc. Exp. Biol. 24 (Part 3)*, S-12–S-23.

Suurkuusk, J., Alvarez, J., Freire, E., & Biltonen, R. (1977) *Biopolymers 16*, 2641–2652.

Turner, D. H., Flynn, G. W., Sutin, N., & Beitz, J. V. (1972) *J. Am. Chem. Soc. 94*, 1554–1559.

Turner, D. H., Yuan, R., Flynn, G. W., & Sutin, N. (1974) *Biophys. Chem. 2*, 385–389.

Zimm, B. H., & Bragg, J. K. (1959) *J. Chem. Phys. 31*, 526–535.